TURBULENCE PATCHES AND FINITE-AMPLITUDE INTERNAL WAVES IN STRATIFIED FLUID WITH STABLE SHEAR

Hieu T. Pham[*], **Sutanu Sarkar**[†]
Department of Mechanical and Aerospace Engineering
University of California, San Diego
9500 Gilman Dr., La Jolla, CA, 92093, USA

Kraig B. Winters[‡]
Scripps Institution of Oceanography
University of California, San Diego
9500 Gilman Dr., La Jolla, CA, 92093, USA

ABSTRACT

Direct Numerical Simulation is performed to investigate the evolution of internal waves and turbulence inside a stratified medium with stable background shear. The upper-ocean flow consists of a shear layer associated with a sub-surface jet located below a free-slip surface. Inside the shear layer, a well-mixed layer is located on top of a linearly stratified layer in which the gradient Richardson number is larger than 0.25. Holmboe instability is observed to grow at the base of the mixed layer, eject thin wisps of heavy fluid into the mixed layer and subsequently generate turbulence. Holmboe instability also excites internal waves into the linearly stratified region. The waves propagate downward in the stratified sheared medium and are reflected upward when the background velocity is too large to support propagating internal waves according to linear wave theory. Intermittent bursts of turbulence with the dissipation rate of at least two orders of magnitude larger than that of the waves are observed in the linearly stratified region. Horseshoe vortices originated from the mixed layer penetrating downward are found to cause the bursts.

MOTIVATION

Shear instability, internal waves and turbulent mixing are intertwined in many geophysical flows. The breaking of large-scale internal waves due to shear instability when the waves steepen can result in significant mixing. On the other hand, shear instability due to background flow conditions can excite internal waves and simultaneously cause mixing. Understanding how these events relate to one another is of fundamental interest in fluid dynamics and is the subject of this paper.

Previous studies have shown that the nonlinear evolution of the Kelvin-Helmholtz instability (Smyth *et al.*, 2001) and the Holmboe instability (Carpenter *et al.*, 2007) at an interface between two fluid of constant density can induce significant turbulent mixing. Pham *et al.* (2009) further show that the Kelvin-Helmholtz instability can also excite strong internal waves when the fluid is continuously stratified. The energy flux carried by the waves can be up to 33% of the amount expended for mixing. In the present study, we investigate the characteristics of internal waves and turbulent mixing as results of the nonlinear evolution of the Holmboe instability at a density interface between a mixed layer and a layer of linearly stratified fluid with background shear.

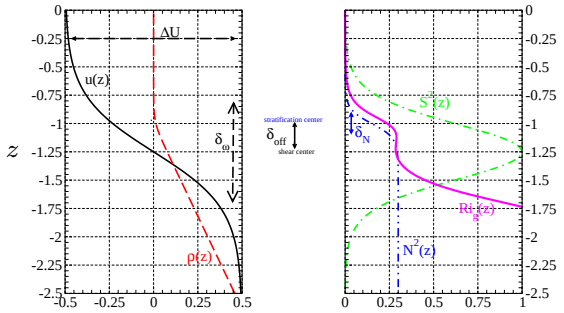

Figure 1: *Initial* mean profiles. The velocity consists of two streams moving in opposite direction with velocity difference ΔU and shear layer thickness, δ_ω. The maximum shear is at $z = -1.25\delta_\omega$. The density variation corresponds to a hyperbolic tangent profile in the squared buoyancy frequency $N^2(z)$. At $z = -\delta_\omega$, $N^2(z)$ transitions from an upper mixed layer to a linearly stratified lower region with the value of N^2 equal to 0.3. The gradient Richarson number Ri_g is less than 0.25 above $z = -1$ and greater than 0.25 in the region below.

FORMULATION

A schematic of the simulated flow is given in Fig. 1: a shear layer between two layers of fluid moving in opposite directions with a velocity difference ΔU and a vertical density stratification owing to a temperature variation. The flow statistics evolve temporally with the assumption that the statistics are homogenous in the streamwise (x) and spanwise (y) directions. The streamwise velocity varies continuously in the vertical cross stream direction (z) with a hyperbolic tangent profile,

$$\langle u \rangle (z, t = 0) = -\frac{\Delta U}{2} tanh\left(\frac{z - 1.25\delta_\omega}{0.5\delta_\omega}\right),$$

where δ_ω is the shear layer thickness. The center of the shear layer is put at $z = -1.25\delta_\omega$ below the surface $z = 0$ to mimick the ocean surface. Here, the bracket $\langle\cdot\rangle$ denotes a horizontal average over the $x - y$ plane. The density $\rho(z, t = 0)$ corresponds to a mixed layer that extends from the surface to depth $z = -\delta_\omega$ where it transitions into a linearly stratified region. The squared buoyancy frequency profile, defined by $N^2 = -(g/\rho_0)\, d\langle\rho\rangle/dz$, has a hyperbolic

[*]h8pham@ucsd.edu
[†]sarkar@ucsd.edu
[‡]kbwinters@ucsd.edu

tangent profile,

$$N^2(z) = \frac{N_d^2}{2} tanh\left(\frac{z-\delta_\omega}{0.5\delta_N}\right),$$

where N_d^2 is a measure of stratification in the region below the shear layer. The thickness, δ_N, of the N^2 profile is 1/4 of the shear layer thickness and the center of N^2 profile is offset $0.25\delta_\omega$ above the center of the shear layer. Profiles of the squared shear rate S^2, the squared buoyancy frequency N^2 and the gradient Richardson number Ri_g are given in Fig. 1 where $S = d\langle u\rangle/dz$ and $Ri_g = N^2/S^2$. Linear stability theory indicates that shear instability occurs in region where $Ri_g < 0.25$. In our setup, shear instability is expected to occur at $z \approx -\delta_\omega$ where the shear is strongest in the region with $Ri_g < 0.25$. Below $z = -\delta_\omega$, although the shear increases, instability is prevented since $Ri_g > 0.25$.

The shear layer thickness δ_ω, the velocity difference ΔU and the stratification in the deep region N_d are used for nondimensionalization. We solve the Navier-Stokes equations under the Boussinesq approximation with the following nondimensional parameters: Reynolds number $Re = \Delta U\delta_\omega/\nu = 5000$, Prandtl number $Pr = \nu/\kappa = 7$, and Richardson number $J_d = N_d^2\delta_\omega^2/\Delta U^2 = 0.3$. Here, ν is the kinematic viscosity, and κ is the molecular diffusivity. Hereafter, the results will be discussed in nondimensional units.

The dimensionless domain size is 8π x 3π x 19.6 and the number of gridpoints in x, y, z directions is 512 x 192 x 256, respectively. The grid is uniform in the streamwise and spanwise directions. In the vertical direction, the grid is stretched from the surface to depth $z = -0.75$ at a ratio of 3% with the smallest grid size of 0.008 at the surface. The grid is uniform in the region $-0.75 > z > -2.5$ with the spacing of 0.02. Below this region the grid is again stretched with a ratio of 3%. A second-order finite difference method on a staggered grid is used for spatial derivatives and a third-order low-storage Runge-Kutta method is used for time advancement. The flow is initialized with low-amplitude velocity perturbations at the density interface. Periodic boundary conditions are used in the x and y directions. A free-slip rigid-lid condition is enforced at the surface $z = 0$ and a Neumann condition is used at the bottom of the domain. A sponge region is employed in the region $z < -10$ to damp out internal waves propagating out of the domain. The simulation includes the linear growth and nonlinear evolution of the Holmboe shear instability resulting in large-scale internal waves and small-scale three-dimensional turbulence. In the following, we discuss these events at length.

HOLMBOE INSTABILITY

The density fields in the vertical plane at $y = 4.7$ in Fig. 2 illustrate the development of Holmboe instability. Carpenter *et al.* (2007) observe that Holmboe instability has slower growth rate compared to Kelvin-Helmholtz instability. In the present study, not until approximately $t = 250$ is the amplitude of the instability large enough to be seen in the density field at $z = -0.9$. The instability has a horizontal wavelength of 8.4 moving with a phase speed of 0.3 in the negative x direction. It is noted that the phase speed is equal to the background velocity $\langle u\rangle$ at the time of instability growth. Hereafter, $z_0 = -0.9$ is used to indicate the depth at which the instability grows.

The nonlinear evolution of the instability is illustrated in Fig. 2(a) with the density field at $t = 346$. On the crests

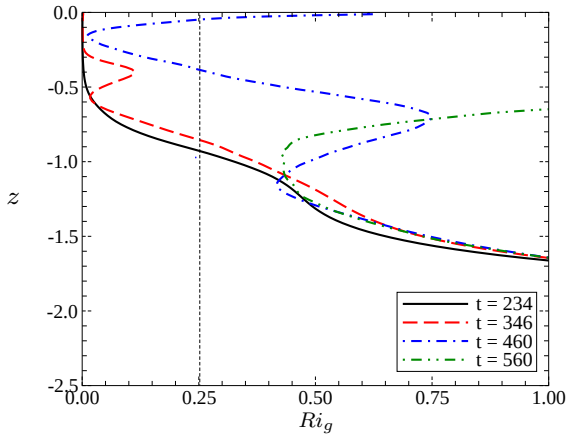

Figure 4: Profiles of Gradient Richardson number Ri_g at various times.

of the instability, thin wisps of heavy fluid are ejected upward into the mixed layer along the direction of the upper stream. Different from Carpenter *et al.* (2007) where the wisps grow freely in the vertical direction, the upward ejections are limited by the presence of the surface at $z = 0$ in the current study. At later time $t = 560$ as shown in Fig. 2(b), the Holmboe instability grows to larger amplitude and the mixed layer becomes turbulent with broadband fluctuations. The interface between the upper turbulent region and lower non-turbulent region is sinusoidal with wavelength of the instability. The vertical location of the interface varies greatly in the x direction. At $x = 10$ the interface is shallow at $z = -0.4$ and at $x = 15$ it reaches deep to $z = -1$. The sinusoidal interface persists even when the turbulence in the mixed layer vanishes at the end of the simulation.

It is interesting to contrast the turbulence interface in the present study with the deepening of a mixed layer by wind-generated or grid-generated turbulence into a stably stratified deep region. In the latter cases, small-scale turbulence erodes the interface and internal waves are radiated. The spatial scales of the radiating waves and that of the largest turbulent eddies are approximately of the same order. As the turbulence subsides, so does the internal wave generation. In the present study, there is a large separation between the two scales. The small-scale turbulent eddies are observed on top of a large-scale sinusoidal interface and the interfacial waves persist longer than the eddies.

The growth of the Holmboe instability extracts momentum from the background mean shear as shown in Fig. 3(a). Between the initial profile in Fig. 1 and one at $t = 234$ in Fig. 3(a), the peak values of S^2 have dropped by 40% due to viscous diffusion of momentum and the instability has not yet grown to finite amplitude. At $t = 346$, the S^2 profile indicates a redistribution of momentum in the mixed layer. In the region $-1.25 < z < -0.6$, S^2 decreases and it is noted that the decrease is due to both viscosity and the Holmboe instability. The difference in S^2 due to viscosity in the region $-2.5 < z < -1.25$ between $t = 234$ and $t = 346$ is smaller than the difference observed in the region above $z = -1.25$. At $t = 346$, the Holmboe instability extracts momentum from the mean shear at z_0, deposits a fraction into the region above and loses a portion in exciting internal waves into the region below. Profiles of S^2 between $t = 346$ and $t = 560$ indicate a significant loss of momentum in the region above $z = -1.25$ while the region below shows insignificant change.

Beside the extraction of momentum, the evolution of the Holmboe instability also alters the background density as

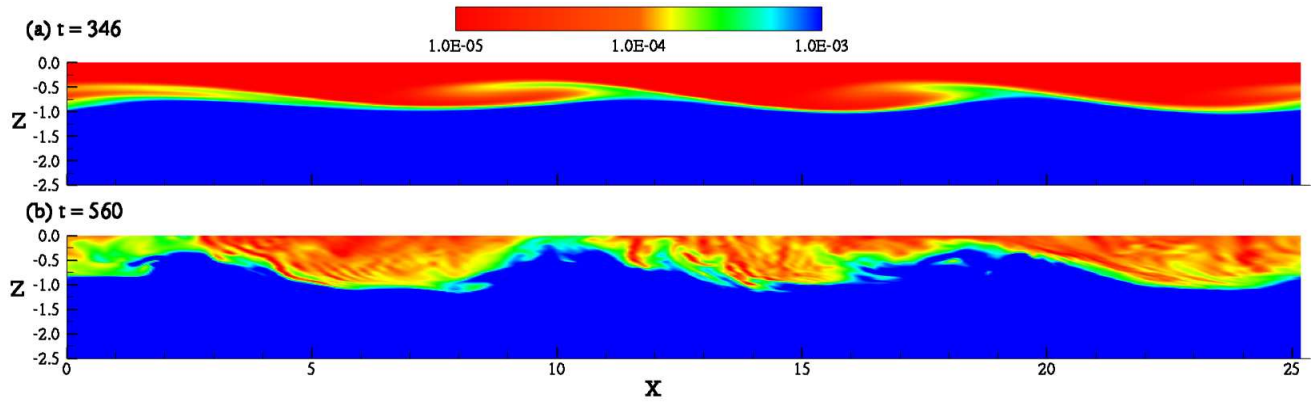

Figure 2: Density fields in the x-z plane at y = 4.7 illustrate the evolution of Holmboe instability: (a) at t = 346 and (b) t = 560.

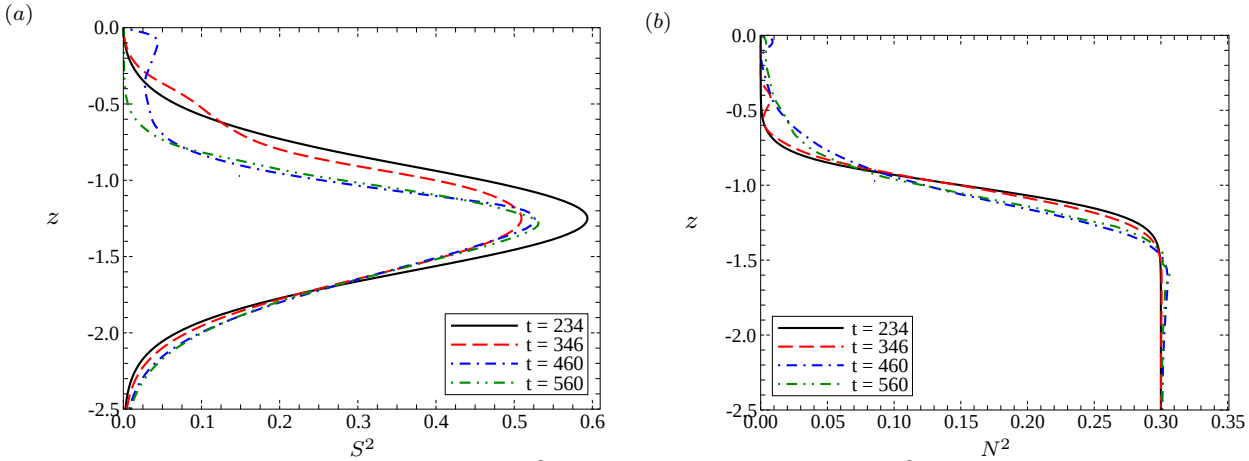

Figure 3: Profiles of squared shear S^2 and squared buoyancy frequency N^2 at various times.

shown in the profiles of N^2 in Fig. 3(b). The formation of the thin wisps ejecting fluid at depth z_0 upward so that the upper region, initially mixed, becomes heavier and N^2 increases. The increase in N^2 in this region also indicates that the turbulence shown in Fig. 2(b) is not strong enough to keep the region well-mixed. Between $t = 346$ and $t = 560$ the stratification in the region $-1.4 < z < -0.9$ decreases suggesting mixing events. The N^2 profiles at $t = 460$ and $t = 560$ have an overshoot in the region $-2.0 < z < -1.4$. An overshoot in N^2 profiles is usually observed when mixing occurs in the immediate vincinity (Sutherland & Linden, 1998; Taylor & Sarkar, 2008). Mixing events in region below z_0 are particularly interesting because the gradient Richardson number Ri_g in this region is always greater than the critical value for linear shear instability as shown in Fig. 4. Over the entire simulation, Ri_g is less than 0.25 only in the mixed layer during the early time. After the Holmboe instability has fully developed and the mixed layer becomes turbulent, Ri_g is greater than 0.25 at all depths. The mixing events in the strongly stratified region are not directly driven by shear instability nor by breaking internal waves and is discussed further in a later section after the following description of internal waves.

INTERNAL WAVES

Internal waves with horizontal wavelength and phase speed equal to that of the Holmboe instability are observed in the sheared region below the depth z_0 as well as in the non-sheared region below $z = -2.5$. The structure of the wave field is shown in Fig. 5 with the fluctuating density ρ'.

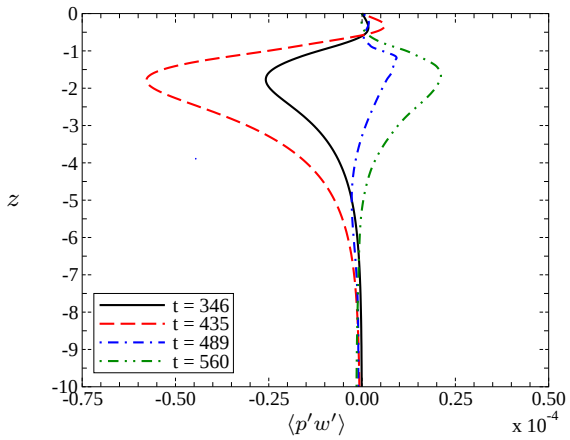

Figure 6: Vertical energy tranpsort by internal waves $\langle p'w' \rangle$ at various times.

Here, the fluctuating field is computed by substracting the horizontally-averaged value from the total value. At $t = 346$, alternating wave crests (red) and troughs (blue) are observed in the region below z_0. The wave structure is vertically coherent with the amplitude being largest near z_0 and followed by rapid decay in the region below $z = -2$. At later time, stronger waves are observed although the structure and the phase speed remain the same. At $t = 560$, the waves reach as deep as $z = -5$ although the amplitude decays quickly with depth.

Linear internal waves can be either propagating or evanescent. Propagating internal waves are known to be able

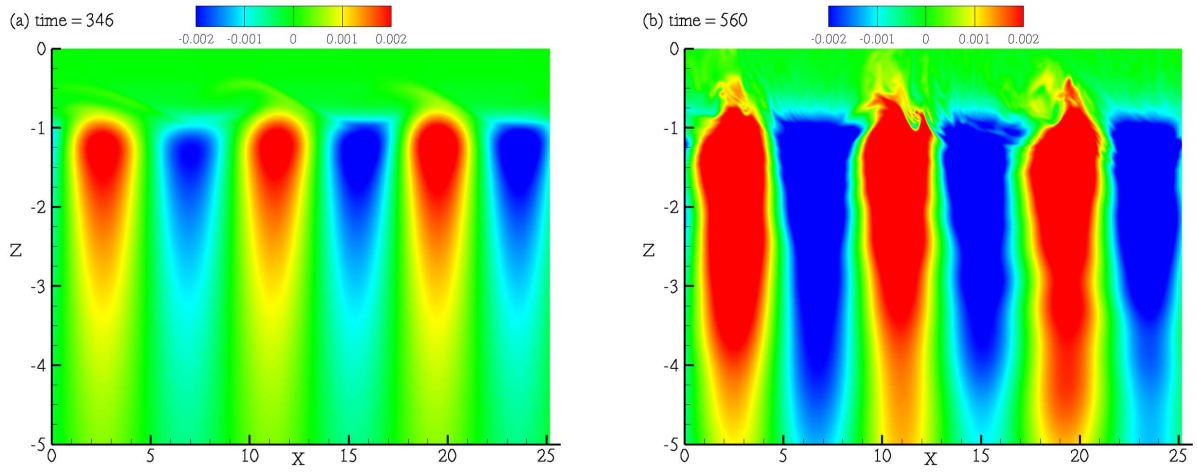

Figure 5: The fluctuating density fields ρ' indicates the presence of internal waves at (a) t = 346 and (b) t = 560.

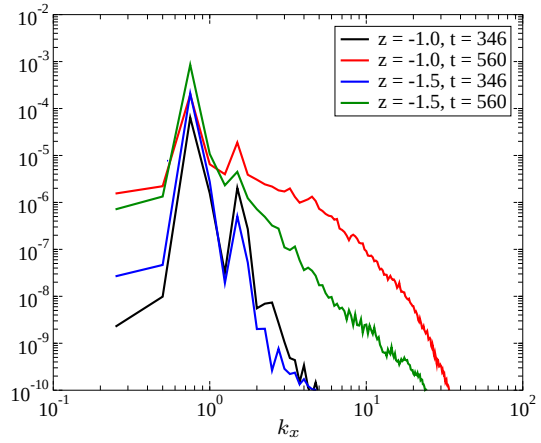

Figure 7: Horizontally-averaged spectra of fluctuating streamwise velociy u' at two depth z = -1 and -1.5 and two different time t = 346 and t = 560.

to distribute momentum and energy in space while evanescent waves have their fluxes decay exponentially in space. It is important to identify the mode of the waves so that the importance of the wave momentum and energy fluxes can be analyzed. The wave energy flux, typically quantified by the pressure-velocity correlation $\langle p'w' \rangle$, is plotted in Fig. 6 at various times. At $t = 346$ and $t = 435$, $\langle p'w' \rangle$ is negative below z_0 indicating that the waves carry energy generated by the Holmboe instability downward. The energy fluxes peak approximately at $z = -1.9$ below which there is no wave propagation. At $t = 489$ and $t = 560$, $\langle p'w' \rangle$ changes signs in the region below z_0, and therefore, the direction of energy tranport is upward during this period. The positive $\langle p'w' \rangle$ in the region $-1.9 < z < z_0$ is indicative of waves reflected at $z = -1.9$ below which linear wave propagation is not possible. The non-negligible values of $\langle p'w' \rangle$ below $z = -1.9$ at late time are associated with the evanescent tail of the internal waves.

Linear wave theory can be used to identify the mode and explain the propagating direction of the internal waves. The theory indicates that for internal waves to propagate in a medium with stratification N, the intrinsic frequency Ω of the waves has to be less than N. When Ω exceeds N, the waves become evanescent. For waves propagating in a continuously sheared medium as in the present study, Ω is equal to $(c - \langle u \rangle) k_x$ where $\langle u \rangle$ is the mean current, c is the wave phase speed in the fixed simulation frame and k_x is the horizontal wavenumber. The horizontally-averaged spectra of the streamwise velocity u' at two different depth and various times in Fig. 7 indicates that k_x is equal to -0.75 where the negative sign corresponds to the wavenumber vector pointing in negative x direction. The phase speed of the wave is equal to the phase speed of the Holmboe instability and thus $c = -0.3$. Since $\langle u \rangle$ varies with depth, the frequency Ω ranges from 0 at z_0 to N at approximately $z = -1.9$ where $\langle u \rangle = c - N/k_x$. Therefore, the waves are propagating between the depth z_0 down to $z = -1.9$ below which the waves are evanescent. Linear wave theory suggests the following: the Holmboe instability grows and excites internal waves at z_0; the waves propagate downward in the stratified sheared medium until $z = -1.9$ where they are reflected upward; below $z = -1.9$ they are evanescent. Later in time, the Holmboe instability decays and the excitation of the internal waves weakens. The signal is dominated by the reflected upward propagating waves. The evolution agrees with the observations in Fig. 5 and 6. It is noted that the waves do not break and they persist until the end of the simulation since they are trapped in the region $-1.9 < z < z_0$.

INTERMITTENT TURBULENCE

The nonlinear evolution of Holmboe instability generates turbulence in the mixed layer as discussed in Carpenter *et al.* (2007); however, in the current study we further observe intermittent bursts of turbulence in region $-1.75 < z < z_0$ where propagating internal waves are observed. Fig. 8 illustrates the dissipation field ε in x-y planes at different depth. Here, the dissipation rate, defined as $\varepsilon = -\nu \left\langle \partial u_i'/\partial x_j \partial u_i'/\partial x_j \right\rangle$, is used to indicate the presence of turbulence. There are localized patches of turbulence in which the dissipation inside the patches is at least two orders of magnitude stronger than in the region outside. The size of the patches are significantly smaller than the wavelength of the internal waves and they are swept by the current in the positive x direction opposite to that of the propagating waves. Although there are more turbulence patches in the plane at depth $z = -1.25$, the patches at depth $z = -1.5$ and -1.75 are correlated with the patches at depth $z = -1.25$ suggesting vertical coherence between the patches. For example, the patches at $x = 12$ and $y = 8$ can be identified at all three depth, and so can the patches at $x = 18$ and $y = 1.5$.

The intermittent bursts of turbulence are not directly related to either linear shear instability or to breaking internal

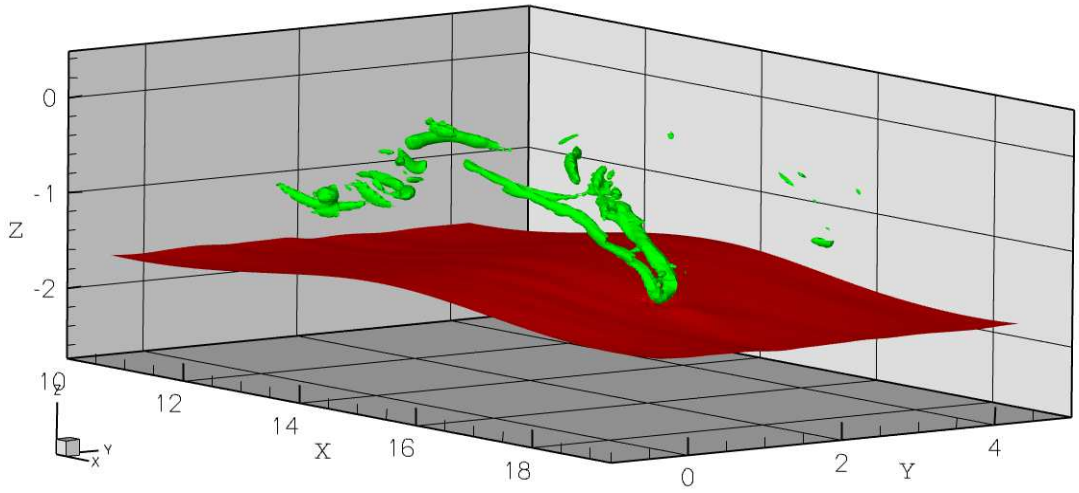

Figure 9: Green horseshoe vortex is shown with $\lambda_2 = -5$ criteria. The red isosurface depicts internal wave with an isopycnal surface of $\rho = .0021$ at $t = 560$.

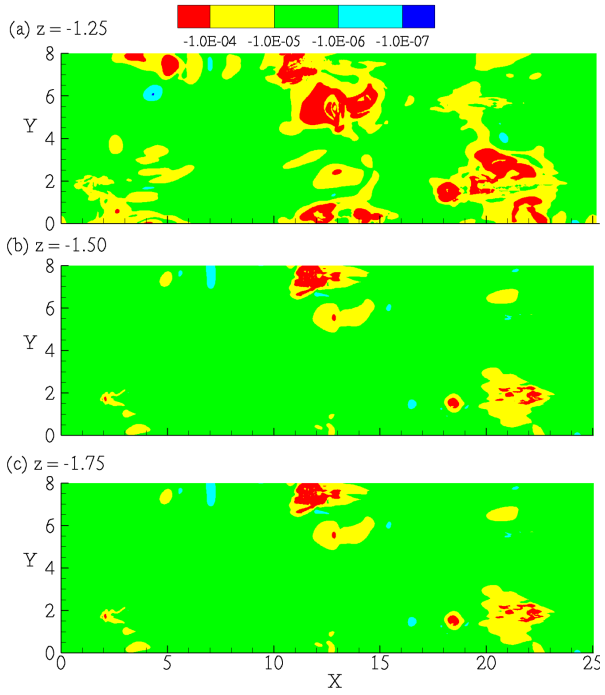

Figure 8: Dissipation rate ε in the x-y plane at t = 463 at three depth (a) z = -1.25, (b) z = -1.5 and (c) z = -1.75.

waves. The bursts are results of the ejections of horseshoe vortex tubes similar to those seen in Pham & Sarkar (2010). Fig. 9 shows the three-dimensional structure of the vortex using the λ_2 criteria which locates the pressure minimum in a plane perpendicular to the vortex axis and accurately defines vortex cores (Jeong & Hussain, 1995). In the figure, the red isosurface is the isopyncal surface of $\rho = 0.0021$ located approximately at depth $z = -1.75$ and the green isosurface of $\lambda_2 = -5$ illustrates the horseshoe vortex. The vortex is formed inside the mixed layer above z_0 and penetrates downward into the region with stable shear below z_0. As the vortex moves downward, it is stretched in the positive x direction forming the horseshoe shape. It is the penetration of these vortices that creates the vertically-coherent intermittent patches of turbulence. In Fig. 9, the tip of the vortex intersects the isopycnal surface creating small-scale turbulence but the structure of the intenal wave is not affected by the vortex. Different from Pham & Sarkar (2010) in which the internal waves disappear after the penetration of the vortices, the internal waves live through in the present study.

The energy budgets of the fluctuating velocities are shown in Fig. 10. In the present study which involves both internal waves and turbulence, the budget is quantified as follows:

$$\frac{dk}{dt} = P - \varepsilon + B - \frac{dT_3}{dz} \,. \tag{1}$$

Here, $k = 1/2 \langle u_i' u_i' \rangle$ is the fluctuating energy, $P = -\langle u'w' \rangle d\langle u \rangle / dz$ is the production rate, $B = -(g/\rho_0) \langle \rho' w' \rangle$ is the buoyancy flux, and ε is the previously-defined dissipation rate. The transport term dT_3/dz is defined with

$$T_3 = \frac{1}{2} \left[\langle w'u'u' \rangle + \langle w'v'v' \rangle + \langle w'w'w' \rangle \right] - \frac{2}{Re_0} \left[\langle u's_{31}' \rangle + \langle v's_{32}' \rangle + \langle w's_{33}' \rangle \right] + \frac{\langle p'w' \rangle}{\rho_0}.$$

In Fig. 10(a), at $t = 346$ the production is the largest source in the budget with a peak at z_0. The Holmboe instability extracts energy from the mean shear and deposits it into the fluctuating fields. The production extends upward to $z = -0.5$ and downward to $z = -2.5$ where the mean shear vanishes. It is important to point out that, at this time when the penetration of the horseshoe vortices has not yet occurred, the production above z_0 is of turbulence while the production below is a signature of internal waves propagating in a sheared medium. Turbulence production has broadband velocity correlation $\langle u'w' \rangle$, also called Reynolds stress, and the background shear is decreased during the turbulence generation as shown in Fig. 3(a). When internal waves travel in a sheared background, their momentum flux, i.e. narrow-band velocity correlation $\langle u'w' \rangle$, in combination with the shear S gives rise to the production. In this case, energy is not extracted from the mean shear and therefore the mean shear is not affected. At $t = 346$, the dissipation is smaller than other components in the budget. The time rate of change in energy dk/dt is positve at all depth. Energy is extracted at z_0 and redistributes in space through the buoyancy flux and the transport.

The budget at $t = 560$ in Fig. 10(b) shows production with negative sign. At late time, the Holmboe instability is

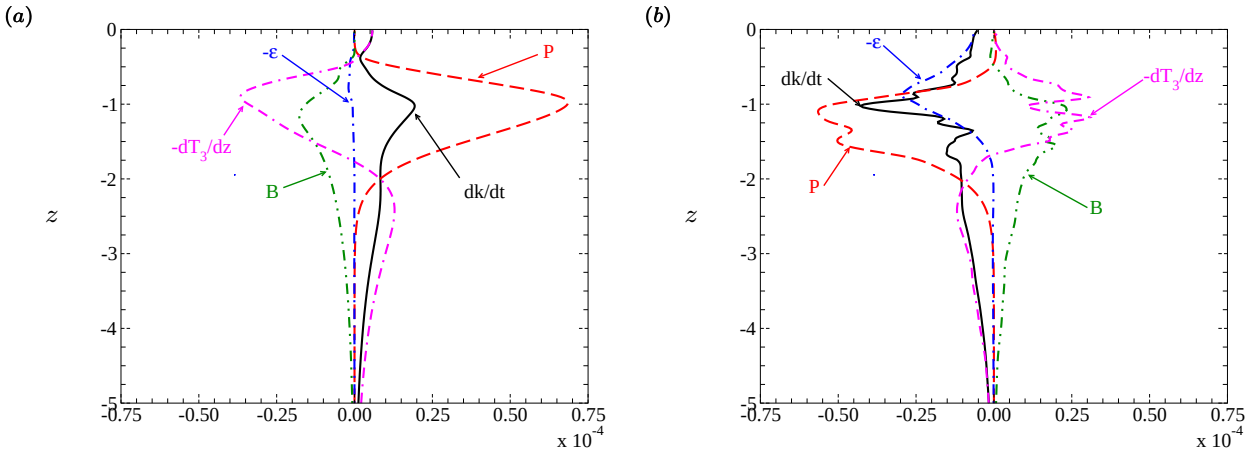

Figure 10: Energy budgets of the fluctuating velocities at (a) t = 346 and (b) t = 560.

shut off since the gradient Richardson is greater than 0.25 and the mixing stabilizes the flow. Energy can no longer be extracted from the mean shear. The negative production indicates that the wave momentum flux $\langle u'w' \rangle$ changes sign as a result of internal wave reflection. As discussed previously, at this time internal waves are reflected at depth $z = -1.9$ carrying energy upward. The dissipation is larger compared to that in Fig. 10(a) with a peak at z_0. The dissipation extends down to depth $z = -1.75$ because the penetration of the horseshoe vortices creates patches of intense turbulence in this region. The source of energy for the dissipation in the region below z_0 can be from the turbulent transport from the region above (turbulent fluxes arriving with the vortices) and the wave energy flux from reflected waves below. Results from Pham & Sarkar (2010) also shows that the horseshoe vortices can further extract energy from the background shear. In the present study, since the internal waves are significantly stronger and persist longer than the turbulence patches, it is difficult to differentiate the energy extracted from the waves from that extracted from the mean shear. The interaction among the vortices, the internal waves and the mean shear deserves more attention in future studies.

CONCLUSIONS

We have used Direct Numerical Simulation to investigate the relationship between shear instability, internal waves and turbulence below a well mixed layer in a stably stratifed shear layer bounded by a free-slip surface. The flow is unique because the stratifcation within the shear layer is set such that there is a small surface mixed layer on top of a larger linearly stratified region. The gradient Richardson number is larger than 0.25 in the linearly stratified region so that linear shear stability is probibited. A Holmboe instability grows at the interface between the mixed layer and the linearly stratified region. The evolution of the Holmboe instability includes Holmboe waves, the ejections of thin wisps of fluid into the mixed layer and finally the generation of turbulence. The instability also excites internal waves. The waves propagate downward from the density interface. At the bottom of the shear layer where the velocity becomes too large to support internal waves, they are reflected upward. Nonlinear evolution of the Holmboe instability creates vortices in the mixed layer. These vortices penetrate down into the linearly stratified region with the background shear. As the vortices come downward, they are stretched into prolonged horseshoe vortex tubes and generate intermittent patches of turbulence. The dissipation inside the turbulence patches is at least two orders of magnitude stronger than that corresponding to the propagating waves. No breaking of the internal waves was observed. The internal waves persist over the entire simulation while the turbulence bursts are short-lived.

REFERENCES

Carpenter, J. R., Lawrence, G. A. & Smyth, W. D. 2007 Evolution and mixing of asymmetric holmboe instabilities. *J. Fluid Mech.* **582**, 103–132.

Jeong, J. & Hussain, F. 1995 On the identification of a vortex. *J. Fluid Mech.* **285**, 64–94.

Pham, H. T. & Sarkar, S. 2010 Internal waves and turbulence in a stable stratified jet. *J. Fluid Mech.* **648**, 297–324.

Pham, H. T., Sarkar, S. & Brucker, K. A. 2009 Dynamics of a stratified shear layer above a region of uniform stratification. *J. Fluid Mech.* **630**, 191–223.

Smyth, W. D., Moum, J. N. & Caldwell, D. R. 2001 The efficiency of mixing in turbulent patches: Inferences from direct simulations and microstrucure observations. *J. Phys. Oceanogr.* **31**, 1969–1992.

Sutherland, B. & Linden, P. 1998 Internal wave excitation from stratified flow over thin barrier. *J. Fluid Mech.* **377**, 223–252.

Taylor, J. R. & Sarkar, S. 2008 Stratification effects in a bottom ekman layer. *J. Phys. Oceanogr.* **38**, 2535–2555.